IOPscience iopscience.iop.org

Home Search Collections Journals About Contact us My IOPscience

Correlation between arsenic precipitates and vacancy-type defects in low-temperature-grown GaAs

This article has been downloaded from IOPscience. Please scroll down to see the full text article.

1994 J. Phys.: Condens. Matter 6 L455

(http://iopscience.iop.org/0953-8984/6/31/006)

View the table of contents for this issue, or go to the journal homepage for more

Download details:
IP Address: 171.66.16.147
The article was downloaded on 12/05/2010 at 19:04

Please note that terms and conditions apply.

J. Phys.: Condens. Matter 6 (1994) L455–L460. Printed in the UK

LETTER TO THE EDITOR

Correlation between arsenic precipitates and vacancy-type defects in low-temperature-grown GaAs

N Hozhabri†‡, J B Bailey†, A R Koymen†, S C Sharma†§ and K Alavi‡
† Department of Physics, The University of Texas at Arlington, Arlington, TX 76019, USA
‡ NSF Center for Advanced Electron Devices and Systems, Department of Electrical Engineering, The University of Texas at Arlington, Arlington, TX 76019, USA

Received 29 April 1994, in final form 2 June 1994

Abstract. We have utilized x-ray photoelectron and variable energy positron beam spectroscopies for depth profiling excess arsenic, arsenic precipitates, and vacancy-type defects in GaAs grown by molecular beam epitaxy at low temperatures (LT-GaAs). XPS results show about 1.3% excess arsenic in as-grown LT-GaAs and a non-uniform depth profile of arsenic concentration in annealed LT-GaAs. Doppler broadening of the positron–electron annihilation radiation (S parameter) reveals a non-uniform depth profile of defects in annealed LT-GaAs. We observe a clear correlation between the depth profile of the S parameter and As in annealed LT-GaAs.

Molecular beam epitaxy (MBE) GaAs grown at low temperatures (LT-GaAs) has been the subject of numerous studies in the last few years. It has been shown that this material contains 1–2% excess arsenic, mostly in the form of As_{Ga} anti-site defects with a density of $\approx 3 \times 10^{19}$ cm^{-3}, and has peculiar optical and electrical properties that are different from those of the normal GaAs that is grown at higher temperatures ($\approx$600 °C) [1–3]. Upon annealing LT-GaAs at temperatures $\geqslant$600 °C, part of the excess arsenic precipitates and forms arsenic clusters [4]. The formation of the arsenic clusters is accompanied by a large increase in the resistivity of the LT-GaAs. When annealed LT-GaAs is used as a buffer layer in GaAs-based devices, it virtually eliminates sidegating or backgating, a common parasitic problem associated with GaAs devices and integrated circuits. In order to explain the peculiar properties of the LT-GaAs, two models have been suggested. One model is based on the formation of spherical buried Schottky barriers associated with arsenic clusters in the annealed LT-GaAs. In this model, the large increase in the resistivity of annealed LT-GaAs is due to overlapping depletion regions of the neighbouring clusters [5, 6]. The second model is based on compensating point defects. In this model, a relatively large number of EL2-like deep-level defects (As_{Ga}) and their role in the hopping conduction account for the anomalous electrical behaviour of the LT-GaAs [7–9].

In this letter, we present depth profiles of arsenic and vacancy-type defects in LT-GaAs by utilizing x-ray photoelectron spectroscopy (XPS) and variable energy positron beam spectroscopy (VEPBS). In the XPS depth profiling technique, the photoelectron spectrum is recorded sequentially after a period of ion beam etching. This process is repeated until the desired depth of the material is exhausted. With this technique, information on the composition and relative concentration of the elements in the sample is obtained in discrete

§ To whom correspondence should be addressed.

0953-8984/94/310455+06$19.50 © 1994 IOP Publishing Ltd

slices throughout the bulk of the sample by monitoring the position and area under designated XPS peaks. Although XPS depth profiling provides unique information about the material, it results in complete destruction of the sample. In contrast, VEPBS is a sensitive but non-destructive technique which also provides valuable information about negatively charged defects and/or vacancy-type defects in semiconductor materials. Due to the lack of ion cores, vacancy-type defects provide an attractive potential to low-energy positrons and consequently trap them. The positron–electron annihilation in a lattice vacancy occurs with low-momentum electrons and thereby produces a relatively small Doppler broadening in the energy spectrum of the annihilation gamma rays. This produces a higher value of the S parameter (defined as the ratio of the area of a central region to the total area under the annihilation gamma-ray peak) and it can be utilized to characterize vacancy-type defects in semiconductors. Details of the interactions of low-energy positrons in semiconductors are discussed elsewhere [10].

The samples used in the present experiments are MBE-grown normal GaAs and LT-GaAs. These were grown in a Varian Gen II modular MBE system on three-inch semi-insulating GaAs mounted on non-indium bonding holders with direct radiation heating at 20 rpm. The growth of the second wafer started within about two hours after the first (unannealed) wafer. Care was taken to grow both LT-GaAs wafers under near identical conditions. In both cases a 1 μm buffer layer of GaAs was grown at normal growth temperature (thermocouple, T/C reading = 700 °C corresponding to 580 °C read by a pyrometer). The growth was then interrupted with the As shutter open the whole time and the substrate temperature was lowered to T/C reading 250 °C. Subsequently, a 1.5 μm layer of LT-GaAs was grown. During the growth of the LT portion of the wafer, the current–voltage was 1.9 A–14 V for the first wafer with T/C reading 247 °C. For the second wafer it was 2.1 A–14 V with T/C reading 246 °C. For both wafers the As oven was at (T/C) 268 °C. The growth chamber pressure during the growth of the LT-GaAs portion of the first wafer was $(1.44–1.48) \times 10^{-8}$ Torr and for the second wafer it was $(1.54–1.57) \times 10^{-8}$ Torr. After the growth of the second wafer, the substrate temperature was quickly ramped to (T/C) 700 °C and the wafer was annealed for one hour (total time including ramping time). Samples were cleaved for VEPBS and XPS from the same area, within a one-inch radius from the centre of each wafer.

In order to investigate the presence of excess arsenic qualitatively, we have performed XPS depth profiling on three samples: normal GaAs, as-grown LT-GaAs, and annealed LT-GaAs. We sputtered the surface of the sample with 3 keV Ar^+ to remove several layers (2 Å min^{-1}) and utilized XPS to monitor the intensities of the $2p_{3/2}$ peaks of As and Ga elements induced by Al-Kα x-rays. Using the standard data analysis techniques, the As concentration in each sample was calculated from [11]

$$C_{As} = \frac{I_{As}/Q_{As}}{I_{As}/Q_{As} + I_{Ga}/Q_{Ga}} \tag{1}$$

where I_{As} and I_{Ga} are linear-background-subtracted areas under the As and Ga peaks and Q_{As} and Q_{Ga} are the quantification factors for As and Ga, respectively. Figure 1 shows the As concentration in the normal GaAs and as-grown and annealed LT-GaAs. The normal GaAs sample shows a uniform spatial distribution of arsenic. The measured data for the normal GaAs are not shown for the purpose of clarity. Instead, they are represented by the dashed line that was obtained from a fit to the measured data. The arsenic concentration in the as-grown LT-GaAs wafer is about 1.3% higher than that in the normal GaAs with a uniform distribution of arsenic in both cases. In contrast, the arsenic concentration in the annealed LT-GaAs has a non-uniform depth distribution. At the surface, the arsenic

concentration is 47% and it approaches 52.1% at a depth of ≈1000 Å. At greater depths, for the range of our XPS study, the arsenic concentration remains at an average value of 52.1%. The arsenic deficiency in the top 800 Å (approximately) of the annealed LT-GaAs is a result of arsenic diffusion from the surface creating a Ga-rich region. Arsenic deficiency in the top region of the annealed LT-GaAs sample is consistent with previous observations made by Smith [2]. Figure 2 shows the concentration of Ga as a function of depth in the annealed LT-GaAs. The top 500 Å thick (approximately) layer of the annealed LT-GaAs has become Ga rich. Although the gallium concentration remains at an average value of 49.5% at a depth of 500 Å, the arsenic concentration (in figure 1) keeps rising for another 500 Å. This difference between the spatial distributions of the Ga and As concentrations is not currently understood. However, it is the VEPBS data (discussed below) that show that these extra gallium atoms in the top 500 Å layer must have occupied vacant sites left behind by diffusing arsenic. Since the total number of the arsenic atoms almost remains the same after annealing the sample, the observed higher value of the arsenic concentration for depths of 1000–3500 Å should be attributed to a higher concentration of arsenic precipitates. The higher concentration of arsenic between 1000 and 3500 Å is due to migration of excess arsenic atoms from near-surface and deeper regions and probably the interfacial region towards the surface.

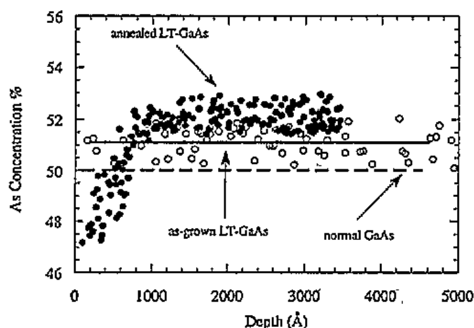

Figure 1. The arsenic concentration versus depth, measured in normal GaAs, as-grown LT-GaAs, and annealed LT-GaAs. The filled and open circles represent the arsenic concentrations for the annealed and as-grown LT-GaAs respectively. The results of the arsenic concentration for normal GaAs have been averaged and shown as a dashed line for clarity.

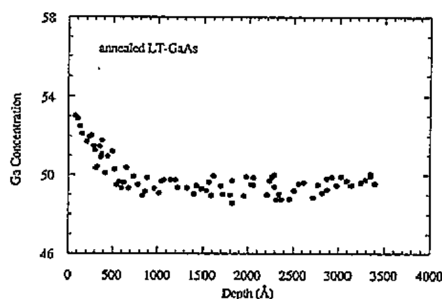

Figure 2. The percentage concentration of Ga ($2p_{3/2}$ XPS peak) as a function of depth in the annealed LT-GaAs.

In addition to performing XPS, we have also measured the *S* parameter in these three samples. The *S* parameters measured for the normal GaAs, as-grown LT-GaAs, and annealed LT-GaAs are shown in figure 3. The constancy of the *S* parameter between the surface and maximum implantation depth of ≈1 μm signals a uniform spatial distribution of defects in as-grown LT-GaAs. In contrast, the *S* parameter in the annealed LT-GaAs shows a non-uniform behaviour. It increases by about 3% (from a normalized value of 1.0 for the normal GaAs) at an implantation depth of ≈800 Å. For mean implantation depths of 800 Å to 5700 Å, the *S* parameter remains constant at 1.03. For implantation depths >5700 Å, the *S* parameter decreases slowly towards 1.01 which is the *S* parameter in the as-grown LT-GaAs. A higher *S* parameter for the as-grown LT-GaAs, in comparison to the *S* parameter for the normal GaAs, is probably due to the presence of a high concentration

of Ga monovacancies [10] and micro-cluster-related defects that are created during the growth of the LT-GaAs. Although As_{Ga} anti-sites and Ga monovacancies are still present in the annealed LT-GaAs, the presence of vacancy complexes or voids associated with arsenic clusters becomes significantly more important in trapping positrons than Ga monovacancies. The trapping of the positrons by As_{Ga} depends on the charge state of these defects. Since some of the As_{Ga} act as donors, they should be positively charged and consequently will not trap positrons. It is also unlikely that positrons are trapped in As_{Ga} with a neutral charge state.

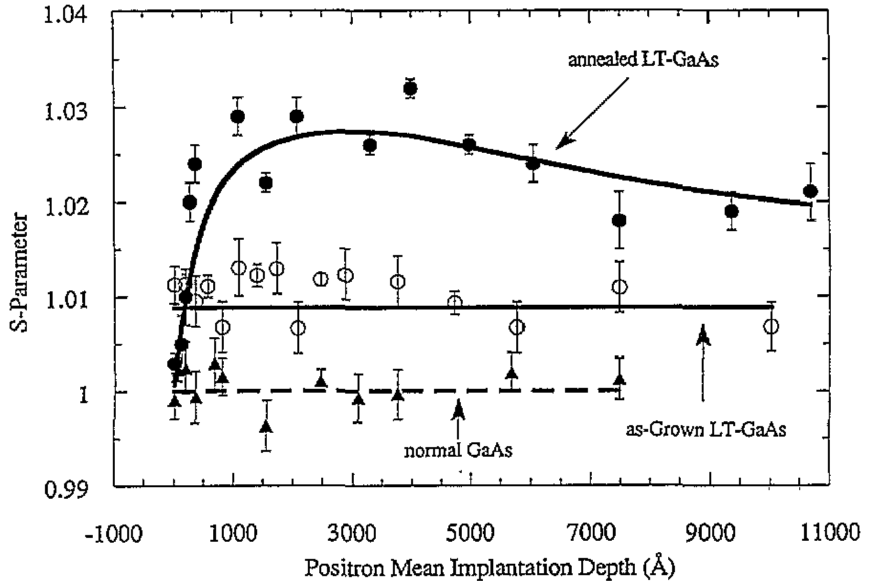

Figure 3. The S parameter versus positron mean implantation depth, measured in annealed LT-GaAs, as-grown LT-GaAs, and normal GaAs. The filled and open circles represent the S parameters for the annealed and as-grown LT-GaAs and filled triangles represent normal GaAs respectively. The error bars represent statistical uncertainties in the S parameter. The solid curve was obtained by fitting the positron diffusion equation to annealed LT-GaAs data.

The similarity between the arsenic concentration and S parameter as functions of depth in annealed LT-GaAs indicates (1) a non-uniform spatial distribution of As-cluster-related defects and (2) trapping of the positrons mainly in vacancy complexes associated with arsenic clusters. Thus the spatial distribution of the S parameter in the annealed LT-GaAs shows spatial distribution of the arsenic clusters in the wafer. This is confirmed by our XPS data. To show the correlation between the measured S parameter and arsenic concentration as a function of depth in annealed LT-GaAs, we have plotted $\Delta S/S_{\mathrm{Surface}}$ versus $\Delta C_{\mathrm{As}}/C_{\mathrm{As\ Surface}}$ in figure 4, where C_{As} is the measured arsenic concentration and deltas represent changes in the S and C_{As} from their surface values. The linear correlation between these two sets of data, obtained from two different techniques, provides the first strong clue to the fact that positrons are probing vacancy-type defects associated with arsenic precipitates in annealed LT-GaAs. This new evidence for the trapping of low-energy positrons in arsenic-cluster-related defects shows that (1) in addition to the presence of Ga monovacancies, vacancy complexes are present in annealed LT-GaAs, (2) these defects are

associated with arsenic clusters, and (3) they are different from V_{Ga} created during the growth and annealing of the sample [12].

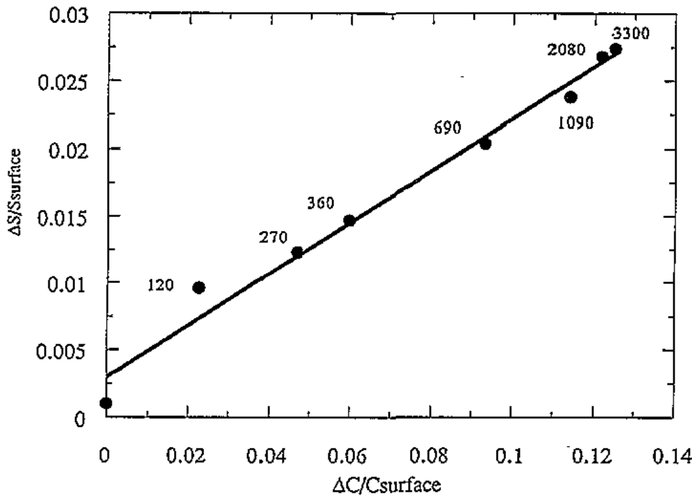

Figure 4. The normalized change in the S parameter versus the normalized change in the arsenic concentration for the annealed LT-GaAs. The numbers associated with data points represent the associated depths in Å.

In conclusion, we have obtained depth profiles of arsenic in as-grown and annealed LT-GaAs samples using XPS. Our XPS results for annealed LT-GaAs show arsenic deficiency near the surface. We have also obtained the depth profile of vacancy-type defects in as-grown and annealed LT-GaAs using VEPBS [13, 14]. From a comparison of the arsenic distribution obtained from XPS and defect profiles obtained by VEPBS in the annealed LT-GaAs, we have shown that (1) the surface region of the annealed LT-GaAs is Ga rich, (2) the vacancy-type defects in annealed LT-GaAs are related to As clusters, and (3) these defects are different from Ga monovacancies.

Research supported in part by a grant from Army Research Office and a grant from the Robert A Welch Foundation.

References

[1] Smith F W, Calwa A R, Chen C L, Manfra M J and Mahoney L J 1988 *IEEE Electron Device Lett.* **EDL-9** 77

[2] Smith F W 1990 *PhD Thesis* MIT, Cambridge

[3] Look D C, Walters D C, Manasreh M O, Sizelove J R, Stutz C E and Evans K R 1990 *Phys. Rev.* B **42** 3578

[4] Melloch M R, Otsuka N, Woodall J M, Warren A C and Freeouf J L 1990 *Appl. Phys. Lett.* **57** 1531

[5] Warren A C, Woodall J M, Freeouf J L, Grischkowski D, McInturff D T, Melloch M R and Otsuka N 1990 *Appl. Phys. Lett.* **57** 1331

[6] McInturff D T, Woodall J M, Warren A C, Braslau N, Pettit G D, Kirchner P D and Melloch M R 1992 *Appl. Phys. Lett.* **60** 448

[7] Look D C, Grant J T and Sizelove J R 1992 *Appl. Phys. Lett.* **61** 1329

[8] Fang Z-Q and Look D C 1992 *Appl. Phys. Lett.* **61** 1438

[9] Look D C, Fang Z-Q, Sizelove J R and Stutz C E 1993 *Phys. Rev. Lett.* **70** 465
[10] Saarinen K, Hautojavri P, Lanki P and Corbel C 1991 *Phys. Rev.* B **44** 10585
[11] Briggs D and Seah M P (ed) 1990 *Practical Surface Analysis* 2nd edn (New York: Wiley)
[12] Ohbu I, Takahama M and Hiruma K 1992 *Appl. Phys. Lett.* **61** 1679
[13] Hozhabri N, Hyer R C, Sharma S C, Ma J Y, Pathak R N and Alavi K 1992 *J. Vac. Sci. Technol.* B **10** 788
[14] Hozhabri N, Sharma S C, Pathak R N and Alavi K 1994 *J. Electron. Mater.* **23** 519